

Toxicity and Pathophysiology of Palytoxin Congeners after Intraperitoneal and Aerosol Administration in Rats

Mark Poli^{1*}, Patricia Ruiz-Olvera¹, Aysegul Nalca², Sara Ruiz², Virginia Livingston², Ondraya Frick², David Dyer², Christopher Schellhase³, Jolynne Raymond³, David Kulis⁴, Donald Anderson⁴, Sara McGrath⁵, Jonathan Deeds⁵

¹*Diagnostic Systems Division, ²Aerobiology Division, or ³Pathology Division, US Army Medical Research Institute of Infectious Diseases, Fort Detrick, Maryland*

⁴*Biology Department, Woods Hole Oceanographic Institution, Woods Hole, Massachusetts*

⁵*Center for Food Safety and Applied Nutrition, US Food and Drug Administration, College Park, Maryland*

*Corresponding author: Diagnostic Systems Division, US Army Medical Research Institute of Infectious Diseases, Fort Detrick, Maryland 21701-5011. mark.a.poli.civ@mail.mil

Opinions, interpretations, conclusions, and recommendations are those of the authors and are not necessarily endorsed by the U.S. Army.

Abstract

Preparations of palytoxin (PLTX, derived from Japanese *Palythoa tuberculosa*) and the congeners 42-OH-PLTX (from Hawaiian *P. toxica*) and ovatoxin-a (isolated from a Japanese strain of *Ostreopsis ovata*), as well as a 50:50 mixture of PLTX and 42-OH-PLTX derived from Hawaiian *P. tuberculosa* were characterized as to their concentration, composition, *in-vitro* potency and interaction with an anti-PLTX monoclonal antibody (mAb), after which they were evaluated for lethality and pathophysiological effects by intraperitoneal (IP) and aerosol administration to rats. Once each preparation was characterized as to its toxin composition by LC-HRMS and normalized to a total PLTX/OVTX concentration using HPLC-UV, all four preparations showed similar potency towards mouse erythrocytes in the erythrocyte hemolysis assay and interactions with the anti-PLTX mAb. The IP LD₅₀ values derived from these experiments (1-3 µg/kg for all) were consistent with published values, although some differences from the published literature were seen. The aerosol LD₅₀ values (.03-.06 µg/kg) confirmed the exquisite potency of PLTX suggested by the literature. The pathophysiological effects of the different toxin preparations by IP and aerosol administration were similar, albeit with some differences. Most commonly affected tissues were the lungs, liver, heart, kidneys, salivary glands, and adrenal glands. Despite some differences, these results suggest commonalities in potency and mechanism of action among these PLTX congeners.

1. Introduction

Palytoxins (PLTXs) are a family of extremely potent marine toxins, considered to be among the most toxic non-proteinaceous substances known. The first member of this family, then called PLTX and now recognized as 42-OH-PLTX (see below), was isolated from the marine coelenterate zoanthid *Palythoa toxica* from a remote tidal pool in Hawaii (Moore and Scheuer, 1971). PLTX congeners have since been described from several additional *Palythoa* species and from dinoflagellates of the genus *Ostreopsis* (Uemura, et al, 1985; Beress, et al, 1983, Oku, et al. 2004). Among the PLTX analogs described from *Ostreopsis* species are the mascarenotoxins A and B from Indian Ocean *O. mascarenensis* (Lenoir, et al 2004), ostreotoxins -1 and -3 from Caribbean *O. lenticularis* (Mercado, et al 1994), and multiple ovatoxins from Mediterranean *O. ovata* (Ciminiello, et al, 2008, 2012a, 2012b). PLTXs are thus found in zooanthids and dinoflagellates distributed throughout tropical and sub-tropical habitats, as well as in temperate waters of the Mediterranean and Adriatic Seas. Further, they have been isolated from seafood (fish, crabs, invertebrates) linked to human illnesses and death, and marine aerosols linked to numerous cases of flu-like symptoms, ocular irritation, and respiratory distress. Finally, PLTXs have been found in high concentrations in marine zooanthids commonly distributed in the home and commercial aquarium trade. Here they have been associated with severe respiratory reactions and corneal damage due to inadvertent contact and the presumed production of aerosols during tank maintenance and cleaning (Deeds, 2014).

The natural production of PLTXs by different organisms demonstrates a certain degree of biological variability. The original structural determination of palytoxin was reported independently by two groups (Moore and Bartolini, 1981; Uemura, et al. 1981), and slight differences in structure and molecular weight were reported for preparations obtained from a Tahitian species of *Palythoa*, Hawaiian *P. toxica*, and Japanese *P. tuberculosa*. PLTX and ovatoxin congeners are minor variations on a common backbone structure (Figure 1, Table 1). Retrospectively, it would appear that the toxin preparations of these two groups may have contained different congeners in different ratios. Our preparation of PLTX from Hawaiian *P. toxica*, originally believed to be pure palytoxin, has since been demonstrated to be almost entirely (>90%) composed of the 42-OH derivative, while another preparation from Hawaiian *P. tuberculosa*, produced concurrently and also originally believed to be pure palytoxin, is now known to be a 50:50 mixture of PLTX and 42-OH PLTX (Ciminiello, et al, 2010). Strains of wild *Ostreopsis ovata* in the northern Adriatic (Accoroni, et al 2011) and cultured *O. ovata* from Brazil (Nascimento et al 2012) have shown ovatoxins-a and -b dominating the toxin profiles, with PLTX present in only trace amounts. Strains of *Ostreopsis siamensis* from Japan produce ostreocin-D, a less potent congener (Ito and Yasumoto, 2009). In all cases, trace amounts of other congeners (i.e. ovatoxins c-k) are nearly always present. Although congeners can be separated using advanced analytical techniques, isolation of pure toxins in high yield is extremely challenging. For this reason, complete structural assignments for all known ovatoxin congeners are not yet possible.

In 1964, using the original semi-purified toxin preparations from Hawaiian *Palythoa toxica*, (based on current knowledge most likely 42-OH PLTX but possibly a mixture of PLTX and 42-OH PLTX) monkeys, dogs, rabbits, guinea pigs, rats, and mice were evaluated by various routes of exposure (Wiles, Vick, and Christensen, 1974). The most potent route was found to be

intravenous, with 24 hr LD₅₀ values ranging from 0.025-0.45 µg/kg depending upon the species tested. LD₅₀ values of 0.24-0.63 µg/kg were observed by the intramuscular, subcutaneous, intraperitoneal and intratracheal routes. Oral and intrarectal routes of exposure were much less toxic. Ito and Yasumoto (2009) confirmed the lower oral toxicity for PLTX and ostreocin-D, but observed bleeding and alveolar destruction in the lungs, gastrointestinal erosion, atrophy in the renal glomeruli, and death within 2 hrs in mice administered 2 µg/kg PLTX and 11 µg/kg ostreocin-D by the intratracheal route.

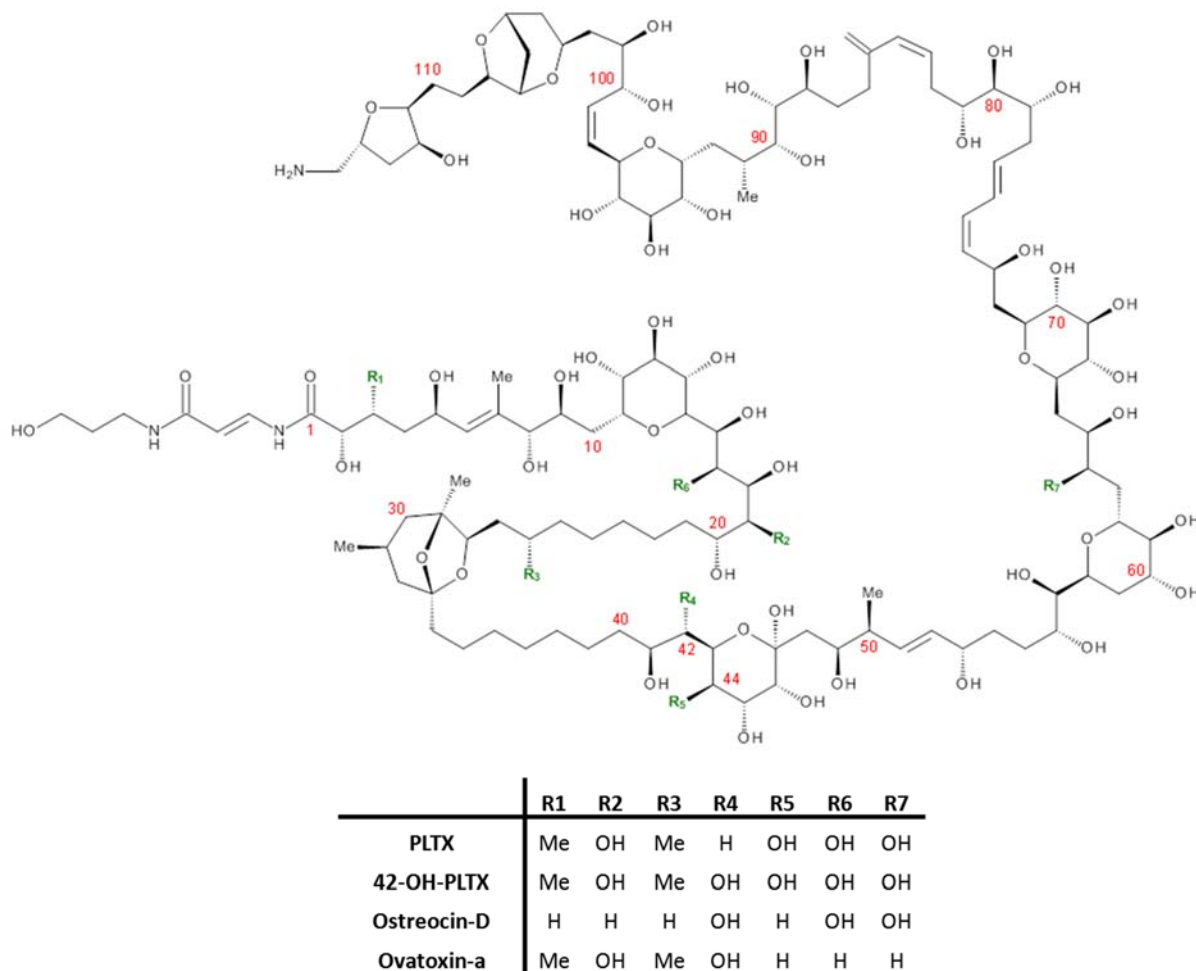


Figure 1. Basic backbone structures of PLTX and the major congeners. (From Pelin, et al., 2016)

Toxin	R1	R2	R3	R4	R5	Other
PLTX	OH	H	OH	OH	OH	
OVTX-a	H	OH	H	OH	H	
OVTX-b	H	OH	H	OH	H	+ C ₂ H ₄ O in region N-C8'
OVTX-c	H	OH	OH	OH	H	+ C ₂ H ₄ O in region N-C8'
OVTX-d	H	OH	OH	OH	H	
OVTX-e	H	OH	H	OH	H	+ O in region C8-C8'
OVTX-f	H	OH	H	OH	H	+ C ₂ H ₄ in region C95-C102
OVTX-g	H	OH	H	OH	H	
OVTX-h	H	OH	H	H	H	Open ring in region C42-C49
OVTX-i	H	OH	H	OH	H	+ C ₂ H ₂ O ₂ – 1 unsaturation in region C49-C52 - O in region C53-C78
OVTX-j1	H	OH	OH	OH	H	+ C ₂ H ₂ O ₂ – 1 unsaturation in region C49-C52 - O in region C53-C78
OVTX-j2	H	OH	H	OH	H	+ C ₂ H ₂ O ₂ – 1 unsaturation in region C49-C52
OVTX-k	H	OH	OH	OH	H	+ C ₂ H ₂ O ₂ – 1 unsaturation in region C49-C52
Isobaric PLTX	H	OH	OH	OH	H	+ O in region C8-C8'

Table 1. Structural modifications of the PLTX backbone comprising the ovatoxins. (From Ciminiello, et al, 2014)

PLTXs are atypical of most known marine toxins in that they pose risks to humans through multiple routes of exposure (oral, inhalational, and dermal) and multiple vectors (planktivorous and carnivorous fish, crustaceans, shellfish, and waters containing *Ostreopsis* cells or zoanthids) (Deeds and Schwartz, 2010). Tubaro et al. (2011) reviewed a series of case reports and anecdotal references describing the adverse effects on human health for different routes of exposure and proposed case definitions for PLTX poisoning. Some of the least studied suspected PLTX exposures involve adverse reactions in humans due to dermal, ocular, and inhalational exposures in persons in close proximity to waters containing blooms of *Ostreopsis* (i.e. swimmers, divers, fisherman), as well as in marine aquarium hobbyists and maintenance workers exposed to toxic zoanthids.

Of particular interest are the observations of acute toxicity following aerosol exposures. One noteworthy example occurred in 2005 when ~ 200 beach-goers experienced symptoms of rhinorrhea, cough, mild dyspnea, bronchoconstriction, and fever that coincided with a bloom of *Ostreopsis ovata* along the Mediterranean coast near Genoa, Italy (Ciminiello, et al, 2006). Some people also experienced conjunctivitis and 20 individuals required extended hospitalization. Altogether, hundreds of cases fitting the description of “Algal Syndrome” have now been reported throughout the northern Mediterranean and Adriatic seas in association with exposure to

waters containing *Ostreopsis ovata* (Durando, et al, 2007). The concentrations of PLTX and/or PLTX-like compounds required to cause these effects are still unknown. These incidents, and many others like them, suggest that PLTXs are a family of toxins that pose a significant risk to humans through aerosol exposure.

The purpose of this study was to characterize four different preparations of PLTX and congeners as to content and purity. Further, we aimed to compare toxicity and basic histopathological effects of each preparation after intraperitoneal (IP) and aerosol administration to rats to better understand differences between congeners. This work is preliminary and supportive of aerosol toxicology studies in nonhuman primates, which will be reported separately. Ultimately, we will develop an animal model for aerosol toxicology of PLTX exposure to be used for testing and evaluation of medical countermeasures.

2. Materials and Methods

2.1 Toxin preparations

Preparation 1, a 50:50 mixture of PLTX/42-OH PLTX, and Preparation 2, containing >90% 42-OH PLTX, were purified previously from Hawaiian *P. tuberculosa* and *P. toxica*, respectively, by the Hawaii Biotechnology Group under contract to the US Army Medical Research Institute of Infectious Diseases (USAMRIID) as reported by Bignami, et al (1992). Preparation 2 was prepared from *P. toxica* obtained from the original tide pool near Hana, on the island of Maui, described by Helfrich (Moore and Scheuer, 1971). Preparation 3 was a commercially available preparation of PLTX (~90-95% pure) purchased from Wako Pure Chemical Industries, Osaka, Japan. Preparation 4 was a mixed ovatoxin preparation containing primarily ovatoxin—a purified from a Japanese strain of *Ostreopsis ovata* (see below).

2.2 *Ostreopsis ovata* culture and purification of ovatoxins

2.2.1 General culture methods

The toxic *Ostreopsis ovata*, strain NIES-3351, was obtained from the National Institute of Environmental Studies, Tsukuba, Japan and was maintained in modified f/2-Si medium (Guillard and Ryther, 1962) as modified by Anderson et al., (1994). The medium was prepared using autoclaved 0.2 µm filtered, UV-irradiated, Vineyard Sound, MA seawater (salinity ~ 32 ppt) for cultures up to 1L which were grown in 2.8L Fernbach flasks. Larger, 17L cultures were grown in sterilized glass carboys filled with sterile nutrient-enriched filtered seawater prior to inoculation with 1L of exponentially growing culture. During incubation, carboys were bubbled with filter- sterilized air supplied by an aquarium pump.

All cultures were maintained at 23 °C on a 14:10 h light:dark cycle (ca. 250 µmol photons·m⁻²·sec⁻¹ irradiance provided by cool white fluorescent bulbs). Cultures were incubated for ~30 days prior to harvest to maximize cellular toxin production (Pezzolesi et al, 2014).

For culture harvest, the contents of individual or multiple Fernbach flasks were added to a tightly capped, pre-weighed vessel that was at least 1L larger in volume than the total culture

harvest volume. The culture was vigorously agitated to free individual cells from the mucous webs that are characteristic of *Ostreopsis* cultures. Clumps of cells varied in size, ranging from 10s to 100s of cells. Without delay, triplicate 1.5 mL aliquot of the dispersed culture were collected and preserved with ~30 μ L Utermohls solution. A minimum of 400 cells were counted using a microscope at 100X total magnification in a Sedgewick-Rafter chamber. Following this, the collection bottle was weighed and this weight, less the empty bottle weight, divided by the density of seawater (1.03g/mL) provided the volume of culture harvested. On average, approximately 7 x 10⁶ cells were contained in each of the harvested 1L volumes of culture. After collection of the cell counts, the culture was filtered through a 13 μ m Nitex sieve to concentrate the cells. Using the filtrate, the cell concentrate was backwashed into a 50mL disposable centrifuge tube which was spun @ 3000 x g for 15 minutes. The overlying seawater was then removed by aspiration. When multiple flasks or carboy volumes of the culture were harvested, the contents were passed through a small (20 cm dia. x 60 cm L) 10- μ m plankton net and the collected cells rinsed into 250mL disposable centrifuge bottles and processed as above. The resulting cell pellet was transferred to 50mL disposable centrifuge tubes and using the same methods as before, concentrated using centrifugation until all the biomass was collected in a single 50mL tube. It was not possible to collect reliable cell count samples from carboy cultures but it is assumed that the cell densities were similar to those quantified in the 1L cultures. All samples were stored at -80 °C following harvest and were shipped on dry ice prior to extraction.

2.2.2 Extraction and purification of ovatoxins

Ten cell pellets, each representing 1 L of culture, were extracted individually with 10 ml of 50:50:0.1 methanol/water/acetic acid following Ciminiello et al. (2012) and Ukena et al. (2001). Each pellet was extracted twice (10 ml each) by sonicating for 1 minute, using a probe sonicator on ice, followed by centrifugation. The extracts were combined (ca. 200 ml total), placed in a 1L glass separatory funnel, and extracted 5 times with 300 ml each of dichloromethane. The remaining de-fatted extract was taken to dryness under vacuum using a rotary evaporator at 30°C to remove any residual dichloromethane. The residue was re-dissolved in 50 ml of extraction solvent and dried again in a rotary evaporator stopping with approx. 5 ml remaining. This final extract was diluted with 20 ml of 50:50 methanol/water and stored at -20°C. At this point the extract was a milky pale yellow color. To clear the solution further for HPLC analysis and fractionation, 10,000 MW spin filters (Amicon® Ultra-15, part# UFC901024, Millipore, Ltd. Carrigtwohill, Ireland) were used, resulting in a clear pale-yellow solution. HPLC analysis with UV detection, following Deeds et al. (2011), of the clear solution revealed that the chromatograms were significantly cleaner after this purification step. For further purification, repeated 200 μ l injections were run over a Gemini C18 column (5 μ m, 110 Å, 150 mm × 2 mm) (Phenomenex, Torrance, CA), with fraction collection, using an Agilent 1200 series HPLC system (Agilent, Wilmington, DE) equipped with an extended injection kit (Part# G1363-68700) and a 1260 Infinity Series fraction collector (Part# G1364C). Samples was eluted using a gradient of 20% solvent A/80% solvent B to 100% solvent A over 10 min at 250 ml/min., followed by a 5 min hold at 100% solvent A at 30 °C [Solvent A: 95% acetonitrile in HPLC grade water/30 mM acetic acid, Solvent B: HPLC grade water/30 mM acetic acid]. Starting gradient conditions were maintained for 5 min. post injection and 10 min. post gradient elution.

PLTX/OVTX-like compounds were determined by their characteristic UV absorbances at 233 and 263 nm. As shown by Ciminiello et al. (2015), this column and elution conditions results in a single combined PLTX/OVTX peak. The OVTX containing peaks were collected, pooled, and re-chromatographed to check purity. The OVTX preparation was finally concentrated under a stream on N₂ at 40°C, adjusted to a concentration of 300 µg/ml with 50:50 methanol/water and quantified using the scheme described below.

2.2.3 Quantification and Characterization of PLTX/OVTX preparations

Toxin preparations were quantified via HPLC with UV detection at 263 nm. Linear regressions were performed in 50:50 methanol/water against a PLTX standard of *P. tuberculosa* purchased from Wako Pure Chemical Industries, Japan. Although not a certified reference standard, this standard is the best characterized commercial preparation available and has been used by others in similar work. Linear regression analysis was performed using GraphPad Prism software (ver. 4.03, GraphPad Prism Software, Inc., San Diego, CA). This method provided a combined concentration of PLTX/OVTX for Preparation 1, 2, and 4. The concentration of Preparation 3, PLTX from *P. tuberculosa* from Wako Pure Chemical Industries, was assumed to be correct.

The four toxin preparations were confirmed as to their identity by liquid chromatography-high resolution mass spectrometry (LC-HRMS) using an Agilent 1290 Infinity UPLC coupled to an Agilent 6538 high resolution qTOF mass spectrometer operating in MS1 mode. Toxins were separated with an Agilent Poroshell 120 EC-C18 column (2.1 x 100 mm, 2.7 um) and a gradient of 28-29 %B over 15 min. at a flow rate of 0.3 mL/min. with mobile phases A = 30 mM acetic acid in water and B = 30 mM acetic acid in acetonitrile, following Ciminiello, et al. (2015). The qTOF recorded all ions eluting from the column and the resultant total ion chromatogram (TIC) was interrogated for ions related to PLTX/OVTXs. .

2.3 In-vitro toxin preparation characterization and cross-reactivity with an anti-PLTX antibody.

2.3.1 Preparation of 73D3 monoclonal antibody (mAb).

The 73D3 mAb producing hybridoma was produced previously by the Hawaii Biotechnology Group under contract to USAMRIID, as described in Bignami, et al. (1992). Hybridoma culture supernatant was diluted 1:10 with 50 mM phosphate buffered saline (PBS) containing 0.02% Tween 20 (PBS/Tween) and circulated over a Protein A/G column (Sigma Chemical Co., St. Louis, MO) at 1 mL/min for the equivalent of 3 sample volumes. After flushing the unbound material off the column with PBS/Tween, the column was eluted with 5 M glycine, pH 3. The IgG peak was collected into an equal volume of 10× PBS, and then dialyzed for at least 16 hr against 5L of distilled water, with 3-4 buffer changes. The dialyzed sample was then lyophilized and stored at room temperature in sealed glass ampules. Prior to use, the lyophilized material was reconstituted with 50mM PBS at 1 mg/mL.

2.3.2 Hemolysis neutralization assay

To compare the *in-vitro* potency of the four toxin preparations, each preparation was first quantified against the PLTX standard from Wako Pure Chemical Industries, Japan (from *P. tuberculosa*), as described above, and prepared as 10 µg/mL stocks in 50:50 methanol/water. Comparative *in-vitro* potency was assessed by hemolysis of mouse red blood cells (RBCs) both with and without the addition of the 73D3 mAb, similar to Bignami (1993). Briefly, whole blood was drawn from strain CD1 female mice using 1.2 mL heparin coated blood collection tubes (S-Monovette®, 1.2ml LH, Sarstedt, Nümbrecht, Germany) following an approved USAMRIID animal care and use protocol. Whole blood was washed three times with ice cold Tris buffer (150 mM NaCl, 3.2 mM KCl, 1.25 mM MgSO₄, and 2.2 mM Tris base, adjusted to pH 7.4 and then 0.22 µm filter sterilized) by suspending in 5 volumes of Tris buffer followed by gentle mixing and centrifugation at 800×g for 5 min., with aspiration of the supernatant. For storage, the final RBC pellet was suspended in two times the original volume using Tris buffer plus 3.75 mM CaCl₂. For the assay, the mouse RBC suspension was diluted 10-fold in Tris buffer plus 1 mM CaCl₂ and 0.5 mM H₃BO₄, for an RBC concentration of 5% of original. To begin the assay, 100 µL of toxin preparation, serially diluted in Tris buffer plus 1 mM CaCl₂ and 0.5 mM H₃BO₄, was mixed in triplicate with either 100 µL of the 5% washed mouse RBC suspension, or the same RBC suspension pre-incubated for 30 min with 25 µg/mL 73D3 mAb, for a final RBC concentration of 2.5% of original. Samples (200 µL total) were mixed in 96 well V-bottom plates, sealed, and incubated for 4 h at 37 °C, after which time plates were centrifuged at 800×g, and 100 µL of supernatant from each well was transferred to a new flat bottom 96 well plate. Absorbance of released hemoglobin was measured at 540 nm using a 96 well plate reader and % hemolysis was calculated through comparison to wells lysed with 10 µg saponin (from Quillaja bark; Sigma Chemical Co., St. Louis, MO).

2.4 Animal studies

2.4.1 Animals

Female Fischer F344 rats were purchased from Charles River Breeding Labs, Frederick MD, and were 5-7 weeks of age at the time of exposure. Animals were housed according to their experimental group and acclimated to their cage mates for at least 7 days prior to initiation of the study. Prior to challenge, rats were implanted subcutaneously with Electric ID Transponder-IPTT 300 (Bio Medic Data Systems, Seaford, Delaware) to measure body temperature and ID. Daily weights were determined on an Adventurer Pro Balance (Ohaus, Parsippany, New Jersey).

2.4.2 Intraperitoneal exposures

Animal research at the United States Army Medical Research Institute of Infectious Diseases (USAMRIID) is conducted under an animal use protocol approved by the USAMRIID Institutional Animal Care and Use Committee in compliance with the Animal Welfare Act, Public Health Service policy, and other Federal statutes and regulations relating to animals and experiments involving animals. The facility where this research was conducted is accredited by the Association for Assessment and Accreditation of Laboratory Animal Care International

(AAALACi) and adheres to principles stated in the Guide to the Care and Use of Laboratory Animals (National Research Council, 2011).

Animals were divided into groups of 8 rats and challenged by IP injection on day 0. The challenge doses were 0.25, 0.5, 1.0, 2.5, and 5.0 µg/kg. Each IP dose was delivered in 100 µL of sterile phosphate buffered saline (PBS), after which the animals were monitored for clinical signs and symptoms twice daily for 7 days. Early intervention endpoints were employed during all studies and rats were humanely euthanized when moribund, according to an endpoint score sheet. Animals were scored on a scale of 0 – 8, with 0-4 being absence of significant clinical signs (e.g. minor changes in fur and movement, stretching of hind limbs, subdued but normal when stimulated), and 5-7 being significant clinical symptoms (ruffled fur, ocular discharge, increased respiration, decreased mobility, subdued even when stimulated). A score of 8 represented moribund animals (greatly labored respiration, gasping, inability to stand, and unresponsive when stimulated). Animals receiving a score of 8 were humanely euthanized via CO₂ exposure followed by bilateral thoracotomy. LD50's were estimated by probit regression, with 95% confidence intervals estimated by delta method approximations in SAS proc NLMIXED SAS version 9.4.

2.4.3 Aerosol exposures

The nose-only exposure was performed by using Automated Bioaerosol Exposure System (ABES II) system. Prior to rat exposures sham aerosols were performed with PLTX/42-OH PLTX from Hawaiian *P. tuberculosa* or 42-OH PLTX from *P. toxica*. The Collison Nebulizer was filled with a 10 mL solution of PLTX/42-OH or 42-OH PLTX, in a vehicle of 1 mg/mL rat albumin and 0.01% acetic acid in 50 mM phosphate buffered saline (PBS). A single all glass impinger (AGI) was prepared with 20 mL PBS and connected to the plenum for each of the sham tests. Each sham test was 15 minutes in duration followed by a five minute wash cycle. The AGI sample was analyzed to determine the aerosol concentration.

Animal inhalation exposures were performed for both dose response and serial sampling studies. For the first and second dose response exposures, Collison Nebulizer concentrations were 40, 8, and 4 µg/mL and 20, 4, 0.8, and 0.16 µg/mL PLTX/42-OH PLTX , respectively. Using the results from these exposures, we optimized the doses for the remaining studies at 8, 6, 4, 2, and 0.8 µg/mL. All test article nebulizer preparations were solubilized in 10 mL PBS, rat albumin, and 0.1% acetic acid. Groups of eight Fisher 344 rats were loaded into the restraint tubes, passed into the BSC, and attached to the plenum. Dose response inhalation exposures were 15-20 minutes in duration followed by a five minute wash cycle. Following the wash cycle, the rats were removed from the plenum and restraint tubes and transported back to their housing room. The AGI samples were collected and stored on ice until they could be assayed. A continuous APS sample was collected for each dose response exposure and analyzed to determine the PSD of the aerosols.

Two groups of 10 Fisher 344 rats were used for each serial sampling study. The Collison Nebulizer concentration was 4 µg/mL for each group.

Inhaled dose was calculated as the product of the aerosol concentration at the breathing zone of the rats on the plenum, minute volume, and exposure duration. Minute volume was estimated using the mean weight of all rats on the day of exposure and Guyton's Equation (1). Aerosol concentration is normally calculated from the measured concentration in the AGI samples. However, due to the extreme potency of these toxins, and the dilution factors inherent

to AGI sample collection, we were unable to directly measure our AGI samples and therefore accurately calculate the exposure doses. Therefore all doses were extrapolated based upon a higher measured dose and therefore estimates. Necessarily, these estimates do not account for run-to-run variation. However, the nose-only inhalation exposure system exhibits excellent linearity and stability and theoretical estimates of concentration closely matched the observed APS particle counts.

The particle size distributions (PSD) of the aerosolized toxins were determined using an APS fitted with an Aerosol Diluter. The mean Mass Median Aerodynamic Diameter and the mean Geometric Standard Deviation (MMAD, GSD) for sham exposures performed with PLTX/42-OH PLTX and 42-OH PLTX were 1.66 μm , 1.73 and 1.08 μm , 2.13, respectively. The mean Mass Median Aerodynamic Diameters and the mean Geometric Standard Deviations (MMAD, GSD) for animal exposures with PLTX/42-OH PLTX, 42-OH PLTX, PLTX, and extracts of toxic *O. ovata* culture were $1.05 \pm 0.03 \mu\text{m}$ ($n = 9$), 2.50 ± 0.20 ($n = 9$), $1.04 \pm 0.01 \mu\text{m}$ ($n = 6$), 2.12 ± 0.09 ($n = 6$), $1.11 \pm 0.04 \mu\text{m}$ ($n = 6$), 2.07 ± 0.28 ($n = 6$), and $1.05 \pm 0.01 \mu\text{m}$ ($n = 6$), 2.22 ± 0.29 ($n = 6$), respectively.

Following the first sham exposure, rat albumin plus 0.1% acetic acid was added to the PBS vehicle to suppress the affinity of PLTXs for glass. This necessarily made the aerosol stickier. Although the test article aerosols were dried and mixed in transit, there was a large particle fraction evident in all PSDs. However, the mass fraction of particles greater than 3.5 μm was insignificant (less than 10%). For all exposures aerosols, at least 87.4% of the particle counts were less than 1.04 μm and at least 99.98% of the particle counts were less than 3.52 μm .

2.4.4 Histopathology

Tissues were collected as soon as possible after death or euthanasia and placed in 10% neutral buffered formalin for a minimum of two days, after which they were submitted for histology. Each sample was trimmed, routinely processed, and embedded in paraffin. Sections of the paraffin-embedded tissues were cut 5 μm thick for histology. Histology slides were de-paraffinized, stained with hematoxylin and eosin (H&E), cover-slipped, and labeled. The study pathologist (CS) reviewed the H&E stained slides of the following tissues: nasal cavity; eyes; ears (middle and inner); pituitary gland, brain (cerebrum and cerebellum); lungs; esophagus; trachea; thymus; lymph nodes (tracheobronchial, mediastinal, mandibular, axillary, inguinal, and/or mesenteric); heart; thyroid gland; liver; spleen; pancreas; stomach; duodenum; jejunum; ileum; cecum/colon/rectum/; right and left kidneys; adrenal glands; ovaries; uterus; urinary bladder; salivary glands; haired skin; femur and/or tibia; skeletal muscle of the hind limb.

3. Results and Discussion

3.1 Characterization of toxin preparations

All four toxin preparations; Preparation 1: a 50/50 mixture of PLTX/42-OH PLTX from Hawaiian *P. tuberculosa*, Preparation 2, 42-OH PLTX from Hawaiian *P. toxica*, Preparation 3: PLTX from *P. tuberculosa* purchased from Wako Pure Chemical Industries, Japan, and Preparation 4: a mixed OVTX preparation containing primarily ovatoxin—a purified from a

Japanese strain of *O. ovata*, were all confirmed as to their identity by LC-HRMS (Figure 2), quantified as to their total PLTX/OVTX concentration by HPLC-UV, and characterized as to their *in-vitro* potency and interaction with the 73D3 mAb through hemolysis neutralization assay (Figure 3).

By LC-HRMS, using the most abundant ion in the spectrum, Preparation 1 was confirmed to be composed of roughly equivalent proportions of PLTX and 42-OH PLTX (observed *m/z* 906.82 for the $[M+H+Ca]^{3+}$ ion for PLTX and *m/z* 912.15 for the $[M+H+Ca]^{3+}$ ion for 42-OH PLTX), Preparation 2 was confirmed to be composed of 42-OH PLTX (observed *m/z* 912.15 for the $[M+H+Ca]^{3+}$ ion), Preparation 3 was confirmed to be composed of PLTX (*m/z* 906.82 for the $[M+H+Ca]^{3+}$ ion), with a second later eluting less abundant peak with the same mass spectra suggesting that this peak is an isomer of PLTX, and Preparation 4 which was confirmed to be composed of OVTX-a (observed *m/z* 896.16 for the $[M+H+Ca]^{3+}$ ion) with lesser amounts of two chromatographically distinct isomeric compounds with observed *m/z* 901.49, for both, identified as $[M+H+Ca]^{3+}$ for OVTX-d and OVTX-e, according to Ciminiello, et al. (2015). It should be noted that the *O. ovata* strain used in this study (NIES-3351 from Japan) was reported previously to produce OVTXs that were identical in molecular weight but distinct in their chromatographic retention times compared to their corresponding OVTX congeners from Italian strains of *O. ovata* (Suzuki et al. 2012). The authors termed these isomers “AC”, or Adachi Culture, derivatives. Since no standards are currently available for the OVTXs, we could not confirm that we produced the AC derivatives of OVTX-a, d, and e, but we assume this to be the case. Previous work using this isolate (identified as strain s-0752 in Suzuki et al. (2012)) found it to produce primarily OVTX-a AC (ca. 85%) with the remainder being roughly equivalent amounts of OVTX-d AC and e AC, with trace amounts of PLTX and OVTX-b AC. With the exception of detecting trace amounts PLTX and OVTX-b AC, this is the same relative toxin composition found in our OVTX preparations. OVTX-a is the 42 hydroxy-17,44,64-trideoxy derivative of palytoxin (Figure 1). OVTX-a AC is reported to be a dideoxy-42-hydroxy-44-deoxy derivative of palytoxin with the 2-unresolved hydroxyl loses occurring between C16 and C20 and C53 and C73, respectively, similar to OVTX-a (Suzuki et al. 2012). This proposed structure has yet to be confirmed through structural elucidation by NMR. The potencies of the Japanese OVTX-AC derivatives compared to their corresponding Italian OVTXs have not been reported.

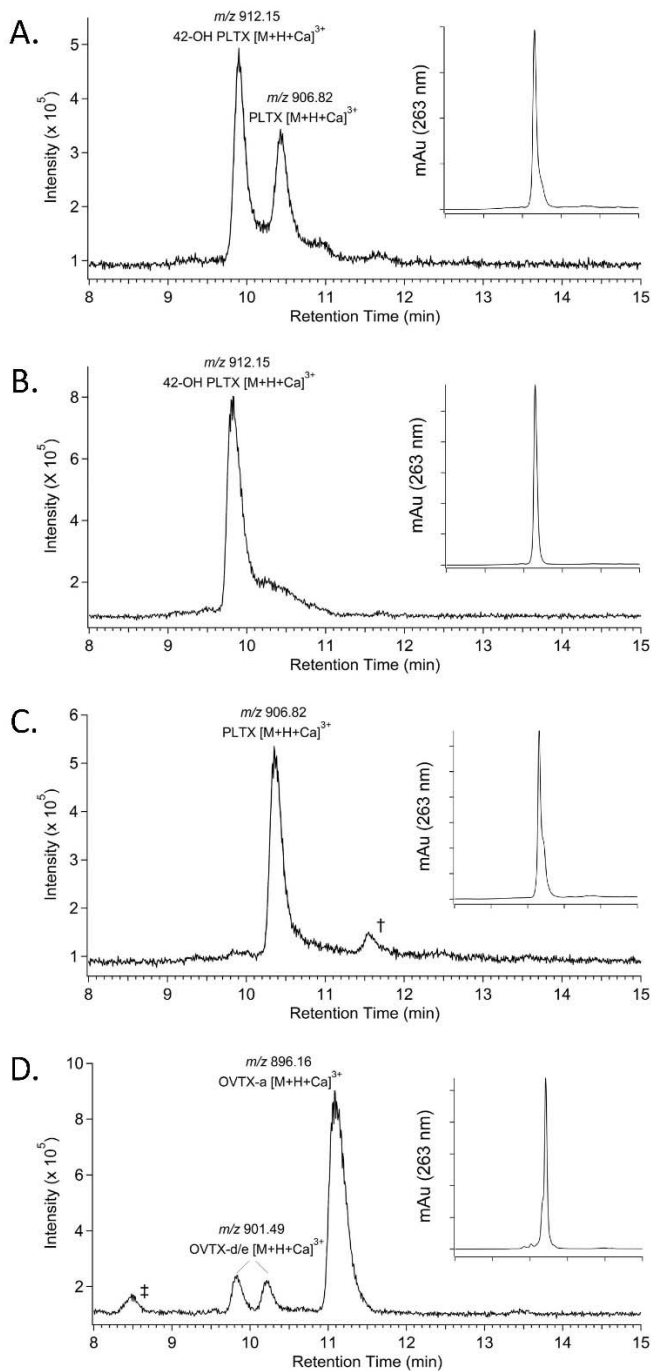


Figure 2. LC-HRMS characterization of toxin preparations used for in-vitro and in-vivo potency assessments. **A.** 50:50 mixture of palytoxin and 42-OH palytoxin from Hawaiian *P. tuberculosa*. **B.** 42-OH palytoxin from Hawaiian *P. toxica*. **C.** Palytoxin from *P. tuberculosa* (purchased from Wako Pure Chemical Industries, Japan). “†” indicates second peak with same mass spectra as first PLTX peak, suggesting the presence of a PLTX isomer. **D.** Ovatoxin prep from *O. ovata* isolate NIES-3351 from Japan. “‡” indicates singly charged contaminant peak that appears to

be unrelated to OVTXs. For all: *m/z* values given were for the most abundant ion observed in the TIC spectra, and inset figure in each panel represents HPLC chromatogram with UV detection at 263 nm used for toxin quantification.

In-vitro potency and comparative interaction with the 73D3 mAb were assessed for the four toxin preparations through the use of a hemolysis neutralization assay. This assay is based upon the potent hemolytic activity of PLTXs towards erythrocytes. The specificity of the activity is confirmed by neutralization by the PLTX-specific mAb. With total PLTX/OVTX concentrations normalized using HPLC-UV, the four toxin preparations showed very similar potency against the mouse RBCs with only the OVTX prep (Preparation 4) showing slightly lower hemolysis across all concentrations (Figure 3). All four toxin preparations were neutralized to similar extents by the 73D3 mAb with hemolytic activity shifted two orders of magnitude at the 50% hemolysis level (Figure 3). The ED₅₀ doses for hemolysis were calculated to be 0.46, 0.37, 0.43, and 0.56 ng/mL for Preparations 1-4, respectively. These potency results are in contrast to those reported by Pelin et al. (2016), who reported a 10-fold difference in potency between ovatoxin-a and PLTX in a similar assay. However, Pelin, et al. (2016) used OVTX-a from Italian strains of *O. ovata*, while we are assuming to have used the OVTX-a AC derivative. In addition, human erythrocytes were used in the Pelin et al. (2016) study, while we used mouse erythrocytes. These two factors, either alone or in combination, could explain these conflicting results.

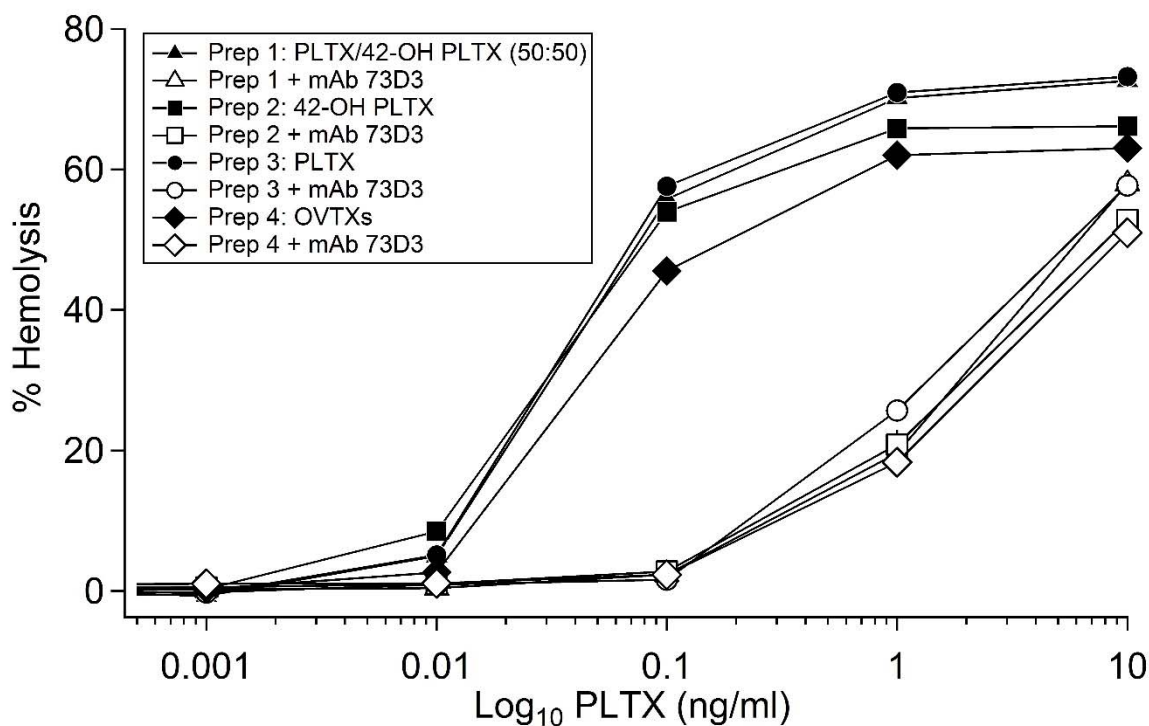


Figure 3. Comparative hemolytic activity against mouse erythrocytes both with and without pre-incubation with 25 µg/mL 73D3 mAb for the four toxin preparations. Prep 1: 50:50 mixture of palytoxin (PLTX) and 42-OH palytoxin (42-OH PLTX) from Hawaiian *P. tuberculosa*. Prep 2:

*42-OH PLTX from Hawaiian *P. toxica*. Prep 3: PLTX from *P. tuberculosa* (from Wako Pure Chemical Industries), Prep 4: ovatoxins (OVTXs) from *O. ovata* strain NIES-3351 from Japan. Symbols are average of triplicate wells, bars represent 1 SD (in most cases bars are smaller than the size of the symbol).*

3.2 Intraperitoneal administration studies

3.2.1 Lethality

The LD₅₀ values calculated from the IP exposures for the four toxin preparations used in this study ranged from 0.92-3.26 µg/kg (Table 2). This data confirms the high potency described in the literature, but differs from other published information in significant ways. Ciminiello et al (2010) demonstrated that the 42-OH PLTX isolated from *P. toxica* used in this study was equipotent with PLTX from Japanese *P. tuberculosa* (from Wako Pure Chemical Industries) in its ability to stimulate Ca⁺⁺ influx in mouse skeletal muscle cells and in its ability to compete for [H³]-ouabain on purified porcine Na⁺/K⁺ ATPase. Tubaro, et al (2011b) also demonstrated equipotency between these preparations in acute oral toxicity studies in mice. However, Ciminiello, et al. (2014) determined that the 42-OH PLTX from *P. tuberculosa* (42S-hydroxy-50R-palytoxin), Preparation 2 in this study, is a stereoisomer of that found in *P. toxica* (42S-hydroxy-50S-palytoxin), contained in our Preparation 1, and had significantly lower potency toward skin HaCaT keratinocytes. This would suggest that Preparation 1 in our study (the 50:50 mix from *P. tuberculosa*) should be less potent than Preparations 2 or 4 (42-OH-PLTX from *P. toxica* or the commercially-available PLTX from *P. tuberculosa*). In fact, differences in potency in our study were minimal, as there was significant overlap in the 95% confidence intervals in our LD₅₀ determinations in rats, and similar hemolytic potencies towards mouse erythrocytes and interaction with the 73D3 mAb. In addition, Pelin, et al (2016) demonstrated that OVTX-a isolated from Mediterranean strains of *O. ovata* had a lower affinity for HaCaT cells, and a corresponding 100-fold lower potency than PLTX in reducing cell viability in the MTT test. While this *in vitro* data suggests that our OVTX-a preparation should be 10-100x less potent than the other preparations, our *in vitro* and *in vivo* data showed minimal differences in both hemolytic activity and lethal potency. One possible explanation for this is that Japanese strains of *O. ovata*, have been reported by Suzuki et al (2012) to produce AC isomers of ovatoxins (explained above). Toxicity comparisons of the AC analogs to the ovatoxins found in the Mediterranean and Adriatic have not yet been made, but it is conceivable that these proposed structural differences could affect potency. Another possibility is that differences may arise from differences between *in vivo* and *in vitro* models used in the various studies.

Other published data in IP exposure to rats is scarce. Our LD₅₀ results differed from than that of Wiles, et al (1974), who reported an IP LD₅₀ in rats of 0.63 µg/kg. However, there were several notable differences between our studies. First, they used a crude toxin preparation from *P. vestitus* (later determined to be *P. toxica*) which was uncharacterized as to both toxin congeners and contamination, and they reported a significantly higher molecular weight (~3300). In addition, they used male rats weighing 200-250 g, while we used female rats weighing approximately 100 g. Whether experimental factors such as these can explain the differences in our results is unknown at this time.

Toxin Prep	Source	LD50 (ug/kg)
50:50 mix	Hawaiian <i>P. tuberculosa</i>	0.92 (0.54 – 1.54)
42-OH-PLTX	Hawaiian <i>P. toxica</i>	1.93 (1.07 – 4.65)
PLTX	Japanese <i>P. tuberculosa</i>	1.81 (1.11 – 3.30)
Ovatoxin-a	<i>Ostreopsis ovata</i> culture	3.26 (2.04 – 5.66)

Table 2. Calculated LD₅₀ values of different palytoxin preparations after intraperitoneal administration to rats. Values are presented as mean and 95% confidence interval.

3.2.2. Histopathology

All euthanized rats were killed by administration of CO₂, followed by bilateral stab incisions of the thoracic wall. This euthanasia method created gross and histologic artifacts including thoracic cavity hemorrhage, pulmonary hemorrhage, hemorrhage/draining hemorrhage in thoracic lymph nodes, and diffuse perivascular and interstitial edema. These artifacts were observed in all euthanized rats to some extent, both nonsurvivors and survivors. However, some nonsurvivor rats had lung pathology not observed in survivors.

Generally speaking, for most tissues, a time lapse of 24 hours or more after tissue injury or death is required before microscopic changes become visible with HE staining; not surprisingly, in nonsurvivors that survived less than four hours (early nonsurvivors), histologic evidence of tissue injury or necrosis was not seen or was rarely observed. Late nonsurvivors (rats that survived over 20 hours PE) developed lesions not seen in early nonsurvivors. Early necrosis and other tissue changes were seen in several tissues in long lived nonsurvivors, and are discussed below.

3.2.2.1 Preparation 1: 50:50 mixture of PLTX and 42-OH PLTX from Hawaiian *P. tuberculosa*

All 40 rats were submitted for histopathologic examination. Twenty-two rats did not survive until end of study (nonsurvivors). Twenty rats were euthanized *in extremis* within three hours PE. One rat was found dead approximately 22 hours PE; one rat was found dead approximately 44 hours PE. The remaining 18 rats survived until end of study (survivors) and were euthanized as described above.

Five rats that survived from 1.6 hr post-exposure (PE) up to 44.3 hr PE had fibrin in the alveolar lumina of the lungs. Two long lived nonsurvivor rats (44 hr and 22 hr) also had increased numbers of alveolar macrophages often with foamy cytoplasmic material (edema or surfactant), or rarely with phagocytized erythrocytes (hemorrhage). One rat also had a focal pulmonary intravascular fibrin thrombus.

Hemorrhagic lesions in the structures of the head were seen in some nonsurvivors; similar lesions were not observed in any survivor rats. Four nonsurvivor rats had either bilateral or unilateral hemorrhage in the middle ear. Middle ear hemorrhage was observed subjacent to

and elevating the epithelial lining of the tympanic cavity. Additionally, one rat had bilaterally symmetrical submucosal hemorrhage in the nasal cavity.

Most (13/22) nonsurvivor rats had acute mild to marked and diffuse draining hemorrhage in the mandibular lymph nodes, suggesting hemorrhage and or venous impairment to structures of the head. No survivors had draining hemorrhage in the mandibular lymph nodes.

The 22 and 44 hr nonsurvivor rats were both found dead and in addition to pulmonary fibrin and hemorrhage, both rats had lesions in other tissues that were not seen in other nonsurvivors. In the liver, both had mild, multifocal, coagulative necrosis of centrilobular hepatocytes. Centrilobular veins in these rats occasionally contained intravascular fibrin or fibrin thrombi. These two rats also had interstitial edema of the pancreas and inflammation and fibrin in the mesenteric fibroadipose tissue. The 44 hour nonsurvivor rat had additional histologic findings of diffuse thymic cortical depletion with lymphocyte necrosis/apoptosis; swelling and degeneration of ducts and acinar cells of the salivary and Harderian glands, as well as lymphoid depletion of the spleen. Only one nonsurvivor had notable renal histopathology consisting of mild, multifocal renal tubular epithelial degeneration and scattered individual cell necrosis; some renal tubular changes in this rat were interpreted as post mortem autolysis. Three survivor rats had multifocal minimal (affecting less than 10% of tissue) regeneration of renal tubules, implying recent tubular injury and repair.

One rat that was found dead had marked bilateral adrenocortical hemorrhage, interpreted as a toxin induced lesion and/or associated with shock. One survivor rat had a focal infarction of the adrenal cortex, the only rat with an adrenal lesion other than hemorrhage.

Several survivors had evidence of peritonitis manifest by diffuse to focal inflammation of the splenic (11/18) and/or hepatic (7/18) capsule and/or the serosa of the stomach or intestines (4/18), which is attributed to IP injection of a toxic or irritant substance.

3.2.2.2 Preparation 2: 42-OH -PLTX from Hawaiian *P. toxica*

In this study, 31/40 rats were submitted for histopathologic examination. Fifteen rats did not survive until end of study (nonsurvivors). Nine of these nonsurvivor rats were euthanized *in extremis* within four hours PE. One rat was euthanized 28 hours PE. The remaining five nonsurvivors were found dead from 23.6 to 28.3 hours PE. The remaining rats (25/40) survived until end of study (survivors) and were euthanized as described above. Sixteen survivors were submitted for histology.

Fibrin, in conjunction with hemorrhage, was observed in the lungs of 4/5 nonsurvivor rats that were found dead (not euthanized). In euthanized rats the extent of pulmonary hemorrhage caused by euthanasia versus PLTX could not be evaluated accurately due to artefactual changes. All late nonsurvivors (6/6) had early/acute coagulative necrosis of hepatocytes in the liver. The distribution was multifocal and random, but typically near centrilobular blood vessels. This lesion was not observed in early nonsurvivors or survivors. Five of 6 late nonsurvivors had renal tubular epithelial degeneration often with necrosis and proteinosis. This lesion was not observed in early nonsurvivors or survivors.

Four nonsurvivor rats had either bilateral or unilateral hemorrhage in the middle ear. Middle ear hemorrhage was observed subjacent to and elevating the epithelial lining of the tympanic cavity. Two survivors had large mature fibrin thrombi in the same location of the middle ear interpreted

as challenge related hemorrhage with progression to mature thrombi by week's end. Four late nonsurvivors had acute unilateral infarction and necrosis of the adrenal gland, and one had acute adrenocortical hemorrhage. This lesion was not observed in early nonsurvivors or survivors. All late nonsurvivors (6/6) had lymphocyte necrosis and lymphoid depletion in the thymic cortex, lymph node(s) and/or spleen. This lesion was not observed in early nonsurvivors or survivors. Six nonsurvivors and most survivors had evidence of peritonitis manifest by diffuse to focal inflammation of the splenic and/or hepatic capsules and/or the serosa of the stomach or intestines.

An interesting finding in 5/15 nonsurvivor rats in this experiment was acute necrosis of salivary gland epithelium, most often of the parotid gland, but also in the submandibular and/or sublingual gland. Several survivors (9/16) had evidence of regeneration of salivary epithelium indicating recent injury to the gland(s). In nonsurvivors for which multiple lymph nodes were examined, most had evidence of hemorrhage and/or draining hemorrhage, especially in thoracic lymph nodes.

3.2.2.3 *PLTX from P. tuberculosa (Wako Standard)*

In this study, 31 rats were submitted for histopathologic examination. Fifteen rats did not survive until end of study (nonsurvivors). Seven of these nonsurvivors were euthanized *in extremis* within four hours PE. Five rats were euthanized approximately 22 hours PE. The remaining 3 nonsurvivors were found dead at 3.6 hours, 3.7 hours, and 46.1 hours PE. The remaining rats (25) survived until end of study (survivors) and were euthanized as described above. Sixteen survivors were submitted for histology.

Three of 6 late nonsurvivor rats that were euthanized and one that was found dead had fibrin in the alveolar lumina, as well as pulmonary hemorrhage and edema. Three late nonsurvivors had histologic lesions consistent with early hepatocyte necrosis. One of these late nonsurvivor rats was found dead at 46 hours PE, and this rat had distinct and extensive areas of coagulative necrosis in the liver. Two survivors had vacuolar degeneration of hepatocytes consistent with sublethal hepatocyte injury. All six late nonsurvivors had some renal tubular epithelial degeneration and scattered individual cell necrosis in the cortices of the kidneys. These lesions were minimal to mild, affecting less than 10% of the cortical tubules. Significant proteinosis (proteinaceous fluid filling tubules, indicating inadequate glomerular and epithelial function) such as that seen in some rats in previous experiments, was not observed in nonsurvivors or survivors in this experiment.

One late nonsurvivor had acute unilateral infarction of the adrenal gland cortex, and three late nonsurvivors had adrenal gland hemorrhage. This lesion was not observed in early nonsurvivors or survivors. All (6/6) late nonsurvivors had lymphocyte necrosis in the thymic cortex, lymph node(s) and/or spleen. This lesion was not observed in early nonsurvivors or survivors. Two nonsurvivors and 9/16 survivors had evidence of peritonitis manifest by diffuse to focal inflammation of the splenic and/or hepatic capsule and/or the serosa of the stomach or intestines. Five nonsurvivors and two survivors had focally extensive, multifocal, or scattered individual cardiomyocytes with acute degeneration characterized by hypereosinophilic cytoplasm indicating that the cell was in a state of hypercontraction at the time it was fixed in formalin.

As with 42-OH-palytoxin, several (5/6) late nonsurvivors had acute necrosis of salivary gland epithelium, most often of the parotid gland, but also in the submandibular and/or sublingual gland. Two survivors had evidence of regeneration of salivary epithelium indicating recent injury to the gland(s). In the two previous experiments using PLTX and the 50:50 mix, many rats had hemorrhage in the middle ear. In this experiment, hemorrhage in the middle ear was not observed in any of the 31 rats examined histologically.

3.2.2.4 Preparation 4: OVTXs from strain NIES-3351 *O. ovata* from Japan

In this study, 27 rats were submitted for histopathologic examination. Nine rats did not survive until end of study (nonsurvivors). Seven of these nonsurvivor rats were euthanized *in extremis* within four hours PE; one was found dead at 3.8 hours PE. One rat was euthanized at 23.3 hours PE. The remaining rats (31) survived until end of study (survivors) and were euthanized as described above. Eighteen survivors were submitted for histology.

Few rats in this experiment had lesions considered relevant to toxin exposure. The lack of histologic lesions in most early nonsurvivor rats is due to the short interval from exposure to death, which was less than 4 hours for 8/9 nonsurvivors. The single nonsurvivor that survived >20 hr did have lesions in several organs/tissues similar to those seen in previous IP experiments including: hemorrhage and fibrin in alveolar lumina of the lungs; infarction of the adrenal gland; acute lymphocyte necrosis in the thymus and spleen; necrosis and degeneration of acinar cells in submandibular and parotid salivary glands. Six nonsurvivors had acute degeneration of myocardiocytes multifocally within the heart; two survivors had similar findings that were interpreted as artifactual change unrelated to any effects of palytoxin. Nine of 18 survivors had inflammation of the mesentery, splenic and/or hepatic capsules. Four survivors had some slight increased incidence of hypercontracted cardiomyocytes. Three survivors had infarction/necrosis of one or both adrenal glands. One rat had extensive necrosis of the parotid salivary gland. One survivor rat, in addition to some degenerative changes in the myocardium, had mild mononuclear inflammation of cardiac muscle in the right ventricle in areas of degenerative .

3.2.1.5 General summary of IP exposure for all toxins

PLTX congeners administered to rats by IP injection caused histologic lesions in several tissues. In this series of experiments most nonsurvivor rats died or were euthanized within a few hours (< 4), before histologically detectable tissue changes could develop. However, in those that survived for 20 hours or longer, toxin induced tissue changes were observed. The most consistently affected organs in nonsurvivor rats were the lungs, liver, salivary glands, adrenal glands, and kidneys. Common nonspecific findings in many rats included lymphoid necrosis and draining hemorrhage. Hypercontraction of cardiomyocytes was observed in a number of rats that did not survive challenge, as well as some survivor rats. Acute cardiomyocyte degeneration due to hypercontraction can be a common background lesion and was observed in nonsurvivors, survivors and negative control rats from this series of experiments. However, it was observed that a few exposed rats that survived until end of study had myocardial inflammation and degenerative changes suggesting that, in addition to damage to the tissues listed above, these toxins also cause injury to cardiac muscle. Subsequent experiments, described below, support this conclusion.

Histologic findings in some organs differed somewhat among the different toxins. PLTX and 42-OH-PLTX caused distinct renal lesions in nonsurvivors including tubular degeneration, necrosis and proteinosis, not seen with ovatoxin-a or the 50:50 mix. For the 50:50 mix, this could reflect the steep dose response curves seen in the lethality studies. Some nonsurvivor rats challenged with the 50:50 mix and 42-OH-PLTX developed acute hemorrhage in the middle ear, and some survivors had organized thrombi in the middle ear indicating recent hemorrhage.

In summary, the IP exposures indicated that the 4 toxin preparations tested were all similar in potency, and the physiological effects, including toxicity to the heart, lungs, kidneys, and lymph nodes, were consistent with previous literature reports (Del Favero, et al, 2013; Ito and Yasumoto, 2009).

3.3 Aerosol exposure studies

3.3.1 Lethality

The LD₅₀ values calculated from the aerosol experiments ranged from 0.031 – 0.063 ug/kg (Table 3). These values are consistent with the extremely high aerosol potency predicted from the intoxication of beachgoers in Italy (Ciminiello, et al. 2006), as well as multiple incidences of exposure to marine aquarists. As discussed above, these doses are estimates, based upon extrapolation of known doses. This was necessary, as our current immunoassays are not sufficiently sensitive to quantitate the small amount of PLTX in the diluted AGI samples captured during the exposure process. As observed with the IP data, there seemed to be little if any difference in potency among the toxin preparations.

Toxin Prep	Source	LD ₅₀ (ug/kg)
50:50 mix	Hawaiian <i>P. tuberculosa</i>	0.063 (0.053 – 0.078)
42-OH-PLTX	Hawaiian <i>P. toxica</i>	0.045 (0.037 – 0.055)
PLTX	Japanese <i>P. tuberculosa</i>	0.041 (0.032 – 0.052)
Ovatoxin-a	<i>Ostreopsis ovata</i> culture	0.031 (0.025 – 0.039)

Table 3. Calculated LD₅₀ values of different PLTX preparations after aerosol administration to rats. Values are presented as mean and 95% confidence interval.

3.3.2 Serial sacrifice studies

Groups of female Fischer 344 rats were administered an estimated aerosol dose of 0.05 ug/kg of each toxin preparation. Sub-groups of rats were then euthanized and necropsied at 0, 12, 24 and 36 hours post-exposure (PE).

3.3.2.1 Gross necropsy results

Gross lesions in rats exposed to aerosolized toxins were similar for all four toxin preparations. Gross lesions, when present, were mostly confined to the lungs and liver, and consisted of pulmonary congestion, lobe consolidation, and/or areas of hemorrhage, and hepatic congestion that occasionally had a lobular pattern. Some rats exhibited epistaxis and/or red crusting around the eyelids and nares.

3.3.2.2 Histopathology

*3.3.2.2.1 Preparation 1: 50:50 mixture of PLTX and 42-OH PLTX from Hawaiian *P. tuberculosa**

In this experiment, 15 rats were exposed. Lesions resulting from this exposure are summarized in Table 4 below. There were no histologic lesions attributed to toxin exposure in rats euthanized immediately after aerosol exposure at T = 0 hr.

At 12 hr PE, 3/4 rats had mild or moderate degeneration and necrosis of the nasal epithelium with accumulation of fibrin, edema and neutrophilic inflammation, and 2/4 rats in this group had degeneration/necrosis of the tracheal epithelium. In the lungs, all 4 rats had moderate perivascular and alveolar fibrin and/or edema, degeneration and necrosis of the epithelium lining the bronchioles with infiltration of neutrophils and macrophages, and an inflammatory infiltrate in the alveolar spaces. In addition to the lesions in the upper and lower respiratory tracts, all rats had moderate (affecting around 50% of examined tissue) necrosis and/or apoptosis of lymphocytes (lymphocytolysis) in the thymus, the spleen, and/or one or more lymph nodes in each rat in this group. Other findings attributed to toxin exposure included degeneration/necrosis of renal distal convoluted tubules (4/4, 100%), ductal degeneration/necrosis in the submandibular salivary gland (2/4, 50%), acinar degeneration/necrosis in the parotid salivary gland (1/4, 25%), minimal degeneration of adrenal gland cortical cells (1/4, 25%), necrotic/apoptotic cellular debris in the small intestine (1/4, 25%) and hemorrhage at the adrenal gland corticomedullary junction (1/4, 25%).

At 24 hr PE, all rats had degeneration and necrosis of the nasal and tracheal epithelium with inflammation. In the lungs, all rats had similar but more severe perivascular and alveolar fibrin and edema, degeneration and necrosis of the bronchiolar epithelium, airway and alveolar neutrophils and macrophages.

Other lesions that were similar between the 12 and 24 hr groups included degeneration/necrosis of renal tubules (4/4), lymphocytolysis in the thymus, spleen and one or more lymph nodes (4/4), degeneration and necrosis of duct epithelium in the submandibular salivary gland (3/3), acinar degeneration/necrosis in the parotid salivary gland (4/4) and degeneration of adrenal gland cortical cells (3/4).

Additional lesions first recognized at 24 hr PE that were not present in the 0 and 12 hr groups included degeneration and necrosis of centrilobular hepatocytes (3/4), and degeneration/necrosis of cardiac myocytes (4/4).

At 36 hr PE, all rats had lesions in the nasal epithelium, trachea, lung, kidney, liver, thymus, spleen, parotid and submandibular salivary glands, heart, thyroid gland, adrenal gland and one or more lymph nodes that were described in earlier groups. The severity varied among the three –being more or less severe than at earlier time points. At 36 hr, 2/3 rats in this experiment had minimal degeneration or necrosis of epithelial cells of the glandular stomach.

(Insert Table 4 here)

Table 4: Results of the aerosol exposure, serial sacrifice experiment using PLTX/42-OH PLTX (50:50 mixture) from Hawaiian *P. tuberculosa*.

3.3.2.2.2 Preparation 2: 42-OH -PLTX from Hawaiian *P. toxica*

In this experiment, 20 rats were exposed. Groups of rats were to be euthanized and necropsied at the following time points after aerosol exposure: 0, 12, 24, and 36 hr. However, except for 4 rats euthanized 0 hr, all remaining rats were euthanized or found dead around 12 hr PE. This likely resulted from dose variability in the aerosolization process between runs, and the steep dose response curve of these toxins in rats. Eleven of the 20 rats were submitted for histologic examination. A summary of the histopathology results is shown in Table 5 below.

Immediately after exposure, 2/4 rats had acute hemorrhage in the nasal cavity; one of these rats had marked, multifocal acute pulmonary hemorrhages. The relationship of these findings to palytoxin is uncertain, as no other rats from other experiments at time point 1 had similar lesions. These observations may be related to toxin exposure, or may be related to the aerosolization procedure or euthanasia. No other histologic lesions related to aerosol exposure or suggestive of toxin exposure were observed in rats at time 0.

At 12 hr PE, all rats had nasal cavity epithelial necrosis and degeneration, and abundant proteinaceous luminal fluid, often with hemorrhage and neutrophilic inflammation. All rats at this time point had lung injury manifest as fibrin exudation into alveolar lumina immediately surrounding larger airways, interstitial and alveolar edema, increased alveolar macrophages and the a mild neutrophilic influx into alveoli. Additional findings in the lungs included necrosis of bronchial and bronchiolar airway respiratory epithelium and alveolar septa with replacement by necrotic debris, neutrophils, many macrophages, fibrin, edema and hemorrhage. Marked congestion of the centrilobular zone of the liver was observed in most rats, and 3/7 rats had mild vacuolar degeneration of centrilobular hepatocytes. Histologic changes of necrosis (pyknosis, hypereosinophilia, loss of differential staining) were not observed in the liver of rats in this

experiment. Post-exposure manifestations of toxin exposure in lymphoid tissues included mild to marked lymphocyte necrosis in the thymic cortex, and in the spleen and/or lymph nodes, mild to minimal depletion of germinal centers with scattered lymphocytolysis and prominent tingible body macrophages. Early mild/minimal degeneration of cardiomyocytes in the right ventricle was observed in 4/7 rats, and scattered necrosis of individual cells was observed in 1 rat. Inflammation was not observed in the heart any rats. In the kidneys, degeneration and rare necrosis of distal cortical tubular epithelium was seen in 6/7 rats. Histologic changes in the kidneys of affected rats were minimal to mild at best, and included cytoplasmic swelling and vacuolation, occasional nuclear pyknosis, and detachment from the basement membrane. In the salivary glands, primarily the submandibular glands, 6/7 rats had multifocal mild degeneration and necrosis of duct epithelium.

(Insert Table 5 here)

Table 5: Results of the aerosol exposure, serial sacrifice experiment using 42-OH PLTX from Hawaiian *P. toxica*

3.3.2.2.3 Preparation 3: PLTX from *P. tuberculosa* (Wako Standard)

Fifteen rats were exposed in this experiment. Groups of rats were euthanized and necropsied at 0, 12, 24, and 36 hr. Results are summarized in Table 6 below. No rats euthanized immediately after aerosolization had histologic lesions suggestive of toxin exposure.

At 12 hr PE, all rats had histologic lesions in the lungs. The primary lesions included necrosis of large airway respiratory epithelium, fibrin exudation into alveolar lumina in areas surrounding large airways (secondary bronchi, bronchioles), increased alveolar macrophages, neutrophilic inflammation, and edema. Lung lesions were moderate to marked in severity, affecting 50-75% of the lung area. In 3/3 rats (the head was not examined for rat 2-2) mild or moderate degeneration and necrosis of the nasal epithelium with some neutrophilic inflammation was observed, and 3/4 rats had necrosis, degeneration and/or loss of tracheal respiratory epithelium. Other findings at 12 hr PE included marked congestion of centrilobular zone of the liver in all rats without significant histologic changes in hepatocytes. All rats had some minimal to mild lymphocyte necrosis and/or apoptosis of lymphocytes (lymphocytolysis) and/or depletion in one or more lymphoid tissues examined (thymus, spleen, mesenteric and/or mandibular lymph node). In addition, 3/4 rats had early mild/minimal degeneration and acute necrosis of cardiomyocytes in the right ventricle and/or right papillary muscle, characterized by cytoplasmic pallor, swelling, or hypereosinophilia, and nuclear pyknosis with/without cytoplasmic mineral precipitation. Additional findings in one or more rats were degeneration/necrosis of renal tubular epithelium (3/4), degeneration/necrosis of duct epithelium in the submandibular salivary gland

(3/4), and one rat (2-3) with a focal area of acute myocyte necrosis with mixed cellular inflammation in skeletal muscle of the rear limb.

At 24 hr PE, all rats had lesions in the lungs, nasal cavity, trachea, liver, heart, lymphoid tissues, kidneys and salivary glands similar to those seen at 12 hr PE but with generally greater severity. In the lungs, fibrin exudation was more extensive, alveolar septae were often necrotic with local hemorrhage, and inflammation was more intense with more neutrophils, including degenerative neutrophils in areas of necrosis (suppurative inflammation). In the heart, the right ventricular myocardium and papillary muscle were affected and infiltrates of low numbers of histiocytes, lymphocytes and few neutrophils were observed in areas of cardiomyocyte injury/necrosis. Right myocardial interstitial edema was seen in 1/4 rats. Coagulative necrosis of centrilobular hepatocytes was observed in 3/4 rats; the fourth rat had hypereosinophilic changes of centrilobular hepatocytes interpreted as early/peracute necrosis. Marked to severe centrilobular congestion was seen in all rats at this time point. Other findings at 24 hr PE included degeneration/necrosis of renal tubules (4/4), lymphoid depletion/necrosis in the thymus and one or more lymph nodes (4/4), duct epithelial degeneration and necrosis in the submandibular salivary gland (4/4).

At 36 hr PE, all rats had lesions in the lungs, nasal epithelium, tracheal epithelium (2/2 examined), liver, kidney tubules, submandibular salivary glands, heart, and lymphoid tissue that were described in the 12 and 24 hr groups. The severity in general, was worse than that seen in rats from earlier time points. One rat from this time point had acute unilateral subepithelial hemorrhage in the middle ear cavity.

(Insert Table 6 here)

Table 6: Results of the aerosol exposure, serial sacrifice experiment using PLTX from *P. tuberculosa* (Waco standard)

3.3.2.2.3 Preparation 4: OVTXs isolated from strain NIES-3351 *O. ovata* from Japan

In this experiment, 20 rats were exposed. Groups of rats were then euthanized and necropsied at the following time points after aerosol exposure: 0, 12, 24, 36, and 48 hr. One rat (1-1) died in the exposure tube before toxin exposure and was, in essence, a negative control animal. As opposed to serial sacrifice experiments with the other toxin preparations, in which all rats died/were euthanized by 36 hr PE, 4 rats from this experiment survived to 48 hr PE. Again, this could result from natural dose variability in the aerosolization procedure. Results are summarized in Table 7 below.

Immediately PE, no rats had histologic lesions suggestive of toxin exposure. Histology in the three exposed rats was similar to that seen in the single rat (1-1) that died prior to exposure.

At 12 hr PE, all rats had histologic lesions suggestive of toxin exposure in the lungs. The primary lesions were small amounts of fibrin in alveolar lumina, neutrophilic inflammation in alveolar lumina and interstitial spaces (e.g. perivascular adventitia), increased alveolar macrophages, neutrophilic exudate in bronchi/bronchioles and necrosis of epithelium, perivascular and interstitial edema. Necrosis of alveoli and/or alveolar pneumocytes was present but was rare. In the nasal cavity, 3/4 rats had increased luminal proteinaceous fluid (mucin) and one rat had mild respiratory epithelial degeneration with a luminal neutrophilic exudate. Marked congestion of the centrilobular zone of the liver was observed in 3/4 rats without significant histologic changes seen in hepatocytes; one rat had diffuse hepatic congestion. All rats had some minimal to mild lymphocyte necrosis and/or apoptosis of lymphocytes (lymphocytolysis) and/or mild/minimal depletion in one or more examined lymphoid tissues (thymus, mesenteric and/or mandibular lymph node). In 3/4 rats, early mild/minimal degeneration and acute necrosis of cardiomyocytes in the right ventricle and/or right papillary muscle was observed. Histologic lesions in the heart were characterized by cytoplasmic hypereosinophilia and nuclear pyknosis with occasional cytoplasmic mineral precipitation. Other findings attributed to toxin exposure included duct epithelial degeneration/necrosis in the submandibular salivary gland (2/4).

At 24 hr PE, all rats had lesions in the lungs, nasal cavity, liver, right heart, lymphoid tissues, and salivary glands. Histologic features were significantly more severe than at 12 hr PE in most tissues. Differences in key tissues from the 12 hr time point included more extensive pulmonary fibrin exudation affecting around 50% of the lung in all rats, often diffuse (marked to severe) necrosis of lining epithelium in large and medium sized airways, necrosis of alveolar septae with local hemorrhage, and intense neutrophilic inflammation, including degenerative neutrophils in areas of necrosis (suppurative inflammation), and widespread marked pulmonary and interstitial edema. In the nasal cavity, especially the caudal nasal cavity, there was multifocal to focally extensive necrosis and degeneration of epithelium, abundant luminal fluid and exudate. In 3/4 rats, tracheal luminal necrotic cellular exudate and neutrophils were observed. In the liver, centrilobular congestion was seen in all rats but additionally at this time point vacuolar degeneration of centrilobular hepatocytes was seen in 2/4 rats and early histologic changes suggestive of necrosis were also occasionally observed in these same two rats. In the right ventricular myocardium and papillary muscle, foci of degeneration and necrosis were observed, often with infiltrates of low numbers of neutrophils and histiocytes. At 24 hr PE a high percentage (50-75% estimated) of lymphocytes in the thymic cortex were necrotic.

At 36 hr PE, all rats had lesions in the lungs, nasal epithelium, liver, heart, salivary glands, and lymphoid tissue that were described in the 12 and 24 hr groups, with exceptions discussed below. The severity of tissue injury and inflammation in the lungs and liver was, in general, worse than that seen in rats from earlier time points. In the liver, 2/4 rats had diffuse severe necrosis of centrilobular hepatocytes not seen at/before 24 hr. Also, 1/4 rats had hepatocyte degeneration and early necrosis similar to the 24 hr group, and one rat had minimal/no liver lesions other than centrilobular congestion. All four rats had diffuse severe necrosis of lymphocytes in the thymic cortex. Two rats had mild lesions in the kidneys consisting of degeneration (swelling) of cortical tubular epithelium and one of these rats had individual necrosis of epithelial cells and mild proteinosis. All four rats at 36 hr had degeneration of salivary gland duct epithelium, but 2/4 had necrosis of acinar cells in the parotid salivary glands as well. One rat had mild focal skeletal muscle degeneration/necrosis in the hind limb.

At 48 hr PE, once again, all rats had pulmonary fibrin, inflammation, necrosis and nasal cavity epithelial degeneration/necrosis. One rat had marked centrilobular hepatocyte necrosis, 3/4 had centrilobular hepatocyte degeneration, and 4/4 had centrilobular hepatic congestion. All rats had severe depletion of the thymic cortex, and 2/4 had mild degeneration of salivary gland duct epithelium. Lung lesions were most severe in the 48 hr rats, in particular the intensity of inflammation and widespread tissue destruction. Lung lesions often involved over 90% of individual lung lobes. Fibrin deposits showed histologic evidence of polymerization (maturation), and reparative efforts such as respiratory epithelial hyperplasia in airways and type 2 pneumocyte hyperplasia in alveoli. At this time point, other tissues showed recovery from acute injury (e.g. salivary glands) and reparative efforts such as goblet cell hyperplasia in nasal cavity epithelium, in addition to those noted in the lungs.

(Insert Table 7 here)

Table 7: Results of the aerosol exposure, serial sacrifice experiment using ovatoxins purified from strain NIES-3351 *O. ovata* from Japan

4. Discussion of Histopathologic Observations

Histopathologic findings in rat serial sacrifice experiments were nearly identical using all four toxin preparations when delivered by aerosol. The progression of pathologic lesions in serial sacrifice experiments followed the same pattern of dissemination and worsening severity over time as seen in the LD50 aerosol experiments and, with the exception of lesions in the lungs, the IP injection experiments.

All aerosolized PLTX preparations caused nasal cavity epithelial degeneration and necrosis. In the nasal cavity, respiratory epithelium showed degeneration with scattered necrosis and sloughing at 12 hr which progressed to focally extensive areas of degeneration and necrosis with a neutrophilic infiltrate and luminal exudate composed of neutrophils and proteinaceous fluid by 24 to 36 hr. Some rats had active nasal cavity epithelial degeneration and necrosis at 48 hr, but also recovery/regeneration of injured lining epithelium and an increase in mucin producing goblet cells.

The major effects of aerosolized PLTX on the lungs was fibrin exudation and tissue necrosis and were first evident at 12 hr PE. The pathologic effects of PLTXs on the trachea and lungs were apparent in all rats at 12 hr PE and were initially characterized by degeneration and necrosis of respiratory epithelium in the trachea, bronchi and bronchioles, with epithelial sloughing and variable numbers of neutrophils in the airway lumina. The first evidence of injury to lung parenchyma (i.e. alveoli) was seen at 12 hr and manifest as fibrin exudation into

alveolar lumina immediately surrounding larger airways, respiratory epithelial necrosis in large airways, occasional alveolar septal necrosis, interstitial and alveolar edema, increased alveolar macrophages and the beginnings of a neutrophilic influx into alveoli and interstitial spaces. By 24 to 48 hr, fibrin exudation was widespread to areas distant from peribronchial or bronchiolar, perivascular, and other interstitial spaces. Consistent findings at 24 hr and later included necrosis and loss of alveolar septa and transmural necrosis of large/medium airways, with replacement by necrotic debris, viable and degenerate neutrophils (suppurative inflammation), many macrophages, fibrin, edema and hemorrhage. With the ovatoxins, where four rats survived to 48 hr, most rats had transmural necrosis of large and medium airways and polymerized (mature) fibrin in alveoli. These rats, similar to long-lived survivors in previous LD50 experiments, had lesions of tissue repair in the lungs to include type 2 pneumocyte hyperplasia and, in those bronchioles and bronchi less affected by necrosis, hyperplasia of respiratory epithelium.

The different PLTXs specifically affected the centrilobular zone of the liver. At 12 hr PE, the majority of rats had significant congestion of the centrilobular zone of the liver, interpreted as an early manifestation of hepatocyte injury to this zone of the liver. At 24 hr PE, degeneration of hepatocytes characterized by cytoplasmic swelling and vacuolation specifically in the centrilobular zone was observed in a high number of rats, and frequently histologic changes consistent with early necrosis, including loss of differential staining and hypereosinophilic cytoplasm, was seen. By 36 hr many rats went on to develop diffuse centrilobular hepatocyte necrosis with centrilobular congestion and some hemorrhage, and degeneration of adjacent surviving hepatocytes. Mild neutrophilic inflammation in areas of hepatocyte necrosis was seen in areas of liver necrosis in one of the rats that survived to 48 hr.

The different PLTXs all caused lymphoid tissue necrosis and depletion, especially in the thymus. Post-exposure manifestations of toxin exposure in lymphoid tissue (thymus, spleen and/or lymph nodes) at 12 hr were composed of minimal to mild thinning (depletion) of germinal centers and/or the thymic cortex, with scattered lymphocytolysis and prominent tingible body macrophages. At 24 hr, effects on lymphoid tissue were seen primarily in the thymic cortex, with diffuse apoptosis/necrosis of lymphocytes. At 36-48 hr, all rats had diffuse depletion of the thymic cortex with very little remnant necrotic cellular debris at 48 hr.

The most commonly and/or exclusively affected areas of the heart were the right ventricle and/or right papillary muscles. Some mild myocardial lesions were observed in rats at 12 hr, consisting of scattered foci of acute degeneration with cytoplasmic swelling or vacuoles, or necrosis, characterized by nuclear pyknosis, cytoplasmic hypereosinophilia and/or fragmentation, and often with cytoplasmic mineral. At 24 hr, multifocal to focally extensive areas of myocardial degeneration and necrosis and interstitial edema were observed in the right ventricle/papillary muscle, and by 36 hr and later, low numbers of neutrophils and histiocytes were observed infiltrating areas of cardiomyocyte injury and loss. In the IP experiments, equivocal changes to cardiac muscle were observed and consisted of acute degeneration without hyaline change, overt necrosis or inflammation. However, in aerosol serial sacrifice experiments, and LD50 aerosol experiments, definitive histologic changes to cardiac myocytes were observed fairly consistently at 12 hr and were followed at later time

points in many rats by distinct lesions of myocardial necrosis and inflammation, thus supporting the conclusion that IP administration of PLTX also affects cardiac muscle.

In the kidneys, degeneration and scattered necrosis of proximal cortical tubular epithelium was seen in rats from 12 -36 hr. Histologic changes in most affected rats were minimal to mild at best, and included cytoplasmic swelling and vacuolation, occasional nuclear pyknosis, and detachment from the basement membrane.

In the salivary glands, primarily the submandibular glands, widespread degeneration and necrosis of duct epithelium was seen, as well as swelling of acinar cells. Foci of acinar cell necrosis in the serial sacrifice experiments were rare, but a higher incidence of salivary gland necrosis, especially the parotid gland, was seen in several rats in IP experiments using 42-OH-PLTX, PLTX, and ovatoxins. Survivors of the IP experiments often had regeneration of salivary gland acini and duct epithelium.

Lesions that were observed in a number of rats in the IP experiments that were rarely or not seen in the serial sacrifice aerosol experiments included unilateral or bilateral subepithelial hemorrhage in the middle ear (total of ten rats using the 50:50 mix and 42-OH-PLTX), and adrenal gland necrosis, infarction and/or hemorrhage, seen in a total of 10 rats from the 42-OH-PLTX, PLTX and ovotoxin preparations.

In our experiments, lesions in the gastrointestinal tract and lesions of skeletal muscle degeneration and necrosis were rarely seen, regardless of route of administration, and were mild to minimal in the few affected animals.

5. Conclusions

Palytoxin derived from Japanese *Palythoa tuberculosa*, and the congeners 42-OH-PLTX (from Hawaiian *P. toxica*) and ovatoxin-a (isolated from a Japanese strain of *Ostreopsis ovata*), as well as a 50:50 mix of PLTX and 42-OH-PLTX derived from Hawaiian *P. tuberculosa* were evaluated for lethality and pathophysiological effects after IP and aerosol administration to rats. The LD₅₀ values derived from these experiments (1-3 µg/kg by IP, 0.03 – 0.06 µg/kg by aerosol) confirmed the exquisite potency of these compounds, although some differences from the published literature were seen. In particular, although we saw a slight trend for ovatoxin-a to be slightly less potent than the other congeners, this difference was uniformly small or absent in *in vivo* and *in vitro* models. These results conflict with multiple published reports that ovatoxin-a is 10-100-fold less potent in several *in vitro* models. This may reflect differences inherent to *in vivo* and *in vitro* methods, as *in vitro* models typically reflect a single tissue type and thus offer a restricted view of the pharmacokinetics and metabolism that are significant factors in *in vivo* models. Alternately, it may reflect differences between the ovatoxin-a typically seen in Mediterranean/Adriatic strains of *O. ovata* and the ovatoxin-a (AC) isomer produced by our Japanese strain. In addition, we did not observe differences in potency between the 42-OH-PLTX produced by *P. toxica* (42S-hydroxy-50S-PLTX) and the 42-OH-PLTX produced by *P. tuberculosa* (42S-hydroxy-50R-palytoxin), as suggested by Ciminiello et al (2014). This again may reflect differences between the *in vitro* and *in vivo* systems used.

The pathophysiological effects of the different toxin preparations were similar in both routes of administration. Although some differences were noted between IP and aerosol

administration – most notably in the lungs - these results suggest commonalities in mechanism of action and potency among the PLTX congeners tested here. There is little published information specifically pertaining to IP and aerosol effects of PLTX congeners in rats to which we can compare our data, and what is available is difficult to compare directly due to differences in experimental parameters or methodology. However, the available literature suggests that these toxins affect a wide range of tissues in a variety of species when administered by multiple routes. Most consistently reported are effects on renal, pulmonary, cardiac, and hepatic tissues, which we also observed here. In addition, we observed effects in lymphoid tissues and salivary glands, but little or no effects on skeletal muscle or gastrointestinal tissues.

These preliminary histopathology results were not designed to be an exhaustive study, but instead to confirm activity in our preparations and to help inform model development. We believe our preparations are sufficiently characterized as to content, purity, and activity to move forward with our ultimate goal of evaluating aerosol toxicology in nonhuman primates. It is anticipated that this data will provide useful information to support the associations seen between PLTX/OVTX and their congeners and toxic events in humans due to presumed aerosol exposure. Ultimately, we will develop an animal model to support the development of medical countermeasures.

6. Acknowledgements

This work was supported by the Defense Threat Reduction Agency, through the Joint Program Executive Office for Chemical and Biological Defense, Contract number CB10396. Additional support to DMA and DLK was provided by National Science Foundation (Grant OCE-1314642) and National Institutes of Health (NIEHS-1P50-ES021923-01) through the Woods Hole Center for Oceans and Human Health. The authors also gratefully acknowledge the support of the technical staff in Pathology Division, USAMRIID for collection and preparation of tissue samples for histopathology, and Ashley DeFee and Candice Zodrow for administrative support.

7. References

- Accoroni, S., Romagnoli, T., Colombo, F., Pennesi, C., Gioia Di Camillo, C., Maurini, M., Battocchi, C., Ciminiello, C., Dell'Aversano, C., Dello Iocovo, E., Fattorusso, E., Tartaglione, L., Penna, A. Totti, C. 2011. *Ostreopsis cf. ovata* bloom in the northern Adriatic Sea during summer 2009: Ecology, molecular characterization and toxin profile. *Mar. Poll. Bull.* 62, 2512-2519.
- Anderson, D.M., Kulis, D.M., Doucette, G.J., Balech, E. 1994. Biogeography of toxic dinoflagellates in the genus *Alexandrium* from the northeastern United States and Canada. *Mar. Biol.* 120, 467-478.
- Beress, L., Zwick, J., Kolkenbrock, H.J., Kaul, P.N., Wassermann, O. 1983. A method for the isolation of the Caribbean palytoxin (C-PTX) from the coelenterate (zooanthid) *Toxicon* 21(2), 285-290.
- Bignami, GS, Raybould, T.J.G., Sachinvala, N.D., Grothaus, P.G., Simpson, S.B., Lazo, C.B., Byrnes, J.B., Moore, R.E., Vann, D.C. 1992. Monoclonal antibody-based enzyme linked immunoassays for the measurement of palytoxin in biological samples. *Toxicon* 30, 687-700.
- Bignami, GS. A rapid and sensitive hemolysis neutralization assay for palytoxin. 1993. *Toxicon* 31, 817-820.
- Ciminiello, P., Dell'Aversano, C., Dello Iocovo, E., Fattorusso, E., Forino, M., Grauso, L., Tartaglione, L., Florio, C., Lorenzon, P., De Bortoli, M., Tubaro, A., Poli, M., Bignami, G. 2010. Stereostructure and biological activity of 42-hydroxy-palytoxin: A new palytoxin analogue from Hawaiian *Palythoa* subspecies. *Chem Res. Toxicol.* 22, 1851-1859.
- Ciminiello, P., Dell'Aversano, C., Dell Iocovo, E., Fattorusso, E., Forino, M., Grauso, M., Tartaglione, L., Guerrini, F., Pezzolesi, L., Pistocchi, R., Vanucci, S. 2012a. Isolation and structure elucidation of ovatoxin-a, the major toxin produced by *Ostreopsis ovata*. *J.Am. Chem. Soc.* 134, 1869-1875.
- Ciminiello, P., Dell'Aversano, C., Dello Iocovo, E., Fattorusso, E., Forino, M., Tartaglione, L., Battocchi, C., Crinelli, R., Carloni, E., Magnani, M., Penna, A. 2012b. Unique toxin profile of a Mediterranean *Ostreopsis cf. ovata* strain: HR LC-MSⁿ characterization of ovatoxin-f, a new palytoxin congener. *Chem. Res. Toxicol.* 25, 1243-1252.
- Ciminiello, P., Dell'Aversano, C., Dello Iocovo, E., Forino, M., Tartaglione, L., Pelin, M., Sosa, S., Tubaro, A., Chaloin, O., Poli, M., Bignami, G. 2014. *J. Nat Prod.* 77, 351-357.
- Ciminiello, P., Dell'Aversano, C., Fattoruso, E., Forino, M., Tartaglione, L., Grillo, C., Melchiorre, N. 2008. Putative palytoxin and its new analogue, ovatoxin-a, in *Ostreopsis ovata* collected along the Ligurian coasts during the 2006 toxic outbreak. *J. Am. Soc. Mass. Spectrom.* 19, 111-120.
- Ciminiello, P., Dell'Aversano, C., Fattorusso, E., Forino, M., Magno, G.S., Tartaglione, L., Grillo, C., Melchiorre, N. 2006. The Genoa 2005 outbreak. Determination of putative palytoxin in Mediterranean *Ostreopsis ovata* by a new liquid chromatography tandem mass spectrometry method. *Anal. Chem.* 78, 6153-6159.

- Deeds, J. R.. 2014. Toxicity of palytoxins. From cellular to organism level responses. In: *Toxins and Biologically Active Compounds from Microalgae, Volume 2: Biological Effects and Risk Management*. Rossini GP (Ed.) CRC Press, Boca Raton, FL. pp. 351-378.
- Deeds, J.R., Handy, S.M., White, K.D., Reimer, J.D. 2011. Palytoxin found in *Palythoa* sp. zoanthids (Anthozoa, Hexacorallia) sold in the home aquarium trade. PLoS ONE 6(4), e18235.
- Deeds, J.R., Schwartz, M.D. 2010. Human risk associated with palytoxin exposure. *Toxicology* 256, 150-162.
- Del Favero G, Beltramo D, Sciancalepore M, et al. 2013. Toxicity of palytoxin after repeated oral exposure in mice and *in vitro* effects on cardiomyocytes. *Toxicology* 275, 3-15.
- Durando, P., Ansaldi, F., Oreste, P., Moscatelli, P., Marensi, L., Grillo, C., Gasparini, R., Icardi, G. 2007. *Ostreopsis ovata* and human health: epidemiological and clinical features of respiratory syndrome outbreaks from a two-year syndromic surveillance, 2005-06, in north-west Italy. *Eurosurveillance* 12(23), 1-6.
- Guillard R.R.L. 1973 Division rates. In: Stein JR (ed) *Handbook of phylogenetic methods: culture methods and growth measurements*. Cambridge University Press, Cambridge, p 289–312.
- Guillard, R.R.L., Ryther, J.H. 1962. Studies of marine plankton diatoms. 1. Cyclotella nanaHustedt and Detonula confervacea (Cleve) Gra. *Can. J. Microbiol.* 8, 229- 239.
- Ito, E., Yasumoto, T. 2009. Toxicological evaluation on palytoxin and ostreocin-D administered to mice by three different routes. *Toxicology* 54(3), 244-251.
- Lenoir, S., Ten-Hage, L., Turquet, J., Quod, J.-P., Bernard, C., Hennion, M.-C. 2004. First evidence of palytoxin analogs from an *Ostreopsis mazarenensis* (Dinophyceae) benthic bloom in southwestern Indian Ocean. *J. Phycol.* 40, 1042–1051.
- Mercado, J.A., Rivera-Rentas, A.L., Gonzalez, I., Tosteson, T.R., Molgo, J., Escalona deMotta, G., 1994. Neuro-and myo-toxicity of extracts from the benthic dinoflagellate *Ostreopsis lenticularis* is sensitive to m-conotoxin. *Soc. Neurosci. Abstr.* 20(1), 718.
- Moore, R.E., Bartolini, G. 1981. Structure of palytoxin. *J. Am. Chem. Soc.* 103, 2491-2494.
- Moore, R.E., Scheuer, P.J. 1971. Palytoxin: a new marine toxin from a Coelenterate. *Science* 172: 495-498.
- Nascimento, S.M., Correa, E., Menezes, M., Varela, D., Paredes, J., Morris, S.. 2012. Growth and toxin profile of *Ostreopsis cf. ovata* (Dinophyta) from Rio de Janeiro, Brazil. *Harm. Algae* 13, 1-9.
- Oku, N., Sata, N.U., Matsunaga, S., Uchida, H., Fusitani, N. 2004. Identification of palytoxin as a principle which causes morphological changes in rat 3Y1 cells in the zooanthid *Palythoa aff. margaritae*. *Toxicology* 43(1), 21-25.

- Pelin, M., Forino, M., Brovedani, V., Tartaglione, L., Dell'Aversano, C., Pistocchi, R., Poli, M., Sosa, S., Florio, C., Ciminiello, P., Tubaro, A. 2016. Ovatoxin-a, a palytoxin analog isolated from *Ostreopsis cf. ovata* Fukuyo: Cytotoxic activity and ELISA detection. *Env. Sci. Technol.* 50, 1544-1551.
- Pezzolesi, L., Pistocchi, R., Fratangeli, F., Dell'Aversano, C., Dello Iacovo, E., Tartaglione, L. 2014. Growth dynamics in relation to the production of the main cellular components in the toxic dinoflagellate *Ostreopsis cf. ovata*. *Harmful Algae*, 36, 1-10.
- Suzuki, T., Watanabe, R., Uchida, H., Matsushima, R., Nagai, H., Yasumoto, T., Yoshimatsu, T., Sato, S., Adachi, M. 2012. LC-MS/MS analysis of novel ovatoxin isomers in several *Ostreopsis* strains collected in Japan. *Harmful Algae* 20, 81-91,
- Tubaro, A., Del Favero, G., Beltramo, D., Ardizzone, M., Forino, M., De Bortoli, M., Pelin, M., Poli, M., Bignami, G., Ciminiello, P., Sosa, S. 2011b. Acute oral toxicity in mice of a new palytoxin analog: 42-hydroxy-palytoxin. *Toxicon* 57, 755-763.
- Tubaro, A., Durando, P., Del Favero, G., Ansaldi, F., Icardi, G., Deeds, J., 2011a. Case definitions for human poisonings postulated to palytoxins exposure. *Toxicon* 57, 478-495.
- Uemura, D., Hirata, Y., Iwashita, T. 1985. Studies on palytoxin. *Tetrahedron* 41, 1007-1017.
- Uemura, D., Ueda, K., Hirata, Y., Naoki, H., Iwashita, T., 1981. Further studies on palytoxin. II. Structure of palytoxin. *Tet. Lett.* 22(29), 2781-2784.
- Ukena, T., Satake, M., Usami, M., Oshima, Y., Naoki, H., Fujita, T., Kan, Y., Yasumoto, T. 2001. Structure elucidation of Ostreosin D, a palytoxin analog isolated from the dinoflagellate *Ostreopsis siamensis*. *Biosci. Biotechnol. Biochem.* 65(11), 2585-2588.
- Wiles, J.S., Vick, J.A., Christensen, M.K. 1974. Toxicological evaluation of palytoxin in several animal species. *Toxicon* 12(4), 427-433.